

UC Irvine

UC Irvine Previously Published Works

Title

Demonstration of trapping, motion control, sensing and fluorescence detection of polystyrene beads in a multi-fiber optical trap

Permalink

<https://escholarship.org/uc/item/4jh4b7vv>

Journal

Optics Express, 13(7)

ISSN

1094-4087

Authors

Jensen-McMullin, Cynthia
Lee, Henry P
Lyons, Edward R

Publication Date

2005

DOI

10.1364/OPEX.13.002634

Peer reviewed

Demonstration of trapping, motion control, sensing and fluorescence detection of polystyrene beads in a multi-fiber optical trap

Cynthia Jensen-McMullin, Henry P. Lee

University of California, Irvine, The Henry Samueli School of Engineering, Irvine, CA 92697
jensenc@uci.edu

Edward R. Lyons

Raytheon Space and Airborne Systems, El Segundo, CA 90245

Abstract: We demonstrate a multi-functional optical trap capable of trapping, motion control, position sensing and fluorescence detection of chemically treated polystyrene beads, using off-the-shelf optical components. It consists of two collinearly aligned single-mode fibers separated by a spacing of 130-170 μm for trapping, another single-mode fiber for probing/pumping and a fourth multi-mode fiber for optical detection. The fibers are mounted either on V-grooved Si or PDMS platforms fabricated using microfabrication and molding techniques, respectively. The result represents an important milestone towards a functional integrated trapping platform.

©2005 Optical Society of America

OCIS codes: (170.4520) optical confinement and manipulation, (060.2310) fiber optics, (170.3880) trapping, microfluidic systems

References and links

1. C.L. Kuyper and D. Chiu, "Optical Trapping: A versatile technique for biomanipulation," *Appl. Spectr.* **56**, 300A-312A (2002).
 2. A. Constable, J. Kim, J. Mervis, F. Zarinetchi and M. Prentiss, "Demonstration of a fiber-optical light-force trap," *Opt. Lett.* **18**, 1867-1869 (1993).
 3. E.R. Lyons and G.J. Sonek, "Confinement and bistability in a tapered hemispherical lensed optical fiber trap," *Appl. Phys. Lett.* **66**, 1584-1586 (1995).
 4. E. Sidick, S.D. Collins, and A. Knoesen, "Trapping forces in a multiple-beam fiber-optic trap" *Appl. Opt.* **36**, 6423-6433 (1997).
 5. J. Guck, R. Ananthkrishnan, H. Mahmood, T.J. Moon, C.C. Cunningham and J. Käs, "The optical stretcher: A novel laser tool to micromanipulate cells," *Biophys. J.* **81**, 767-784 (2001).
 6. Y. Ogura, K. Kagawa and J. Tanida, "Optical manipulation of microscopic objects by means of vertical-cavity surface-emitting laser array sources," *Appl. Opt.* **40**, 5430-5435 (2001).
 7. R.A. Flynn, A.L. Birkbeck, M. Gross, M. Ozkan, B. Shao, M.W. Wang and S.C. Esener, "Parallel transport of biological cells using individually addressable VCSEL arrays as optical tweezers," *Sens and Actuat.* **87**, 239-243 (2002).
 8. S. McGreehin, L.O'Faolin, J. Roberts, T. Krauss and K. Dholakia, "Optoelectronic Integrated Tweezers," in *Optical Trapping and Optical Manipulation*, K. Dholakia and G.C. Spalding, eds., *Proc. SPIE* **5514**, 55-61 (2004)
 9. I.A. Vorobjev, H. Liang, W.H. Wright and M. Berns, "Optical trapping for chromosome manipulation: a wavelength dependence of induced chromosome bridges," *Biophys. J.* **64**, 533-538 (1993).
 10. J. Cooper McDonald, D.C. Duffy, J. R. Anderson, D.T. Chiu, H. Wu, O.J.A. Schueller, G.M. Whitesides, "Fabrication of microfluidic systems in poly(dimethylsiloxane), *Electrophoresis* **21**, 27-40 (2000).
 11. E.R. Lyons, "Application of fiber optic techniques to optical trapping," Master's Thesis, University of California, Irvine (1994).
 12. M. Bachman, Y.M. Chiang, C. Chu and G.P. Li, "Laminated microfluidic structures using a micromolding technique," in *Microfluidic Devices and Systems II*, C.H. Ahn and A.B. Frazier, eds., *Proc. SPIE* **3877**, 139-146 (1999).
-

1. Introduction

Optical tweezers based on optical trapping mechanism have become a common tool in medicine and biology. They are widely used for manipulation, diagnosis and alteration of cells, microorganisms and macromolecules [1]. Current commercial optical tweezers, based on the gradient force of a single focused beam in free space tend to be bulky and expensive, and the trapped objective moves in three-dimensional space. It is highly desirable to miniaturize optical traps on a planar platform that is compatible and integratable with low-cost microfluidic chips.

There have been several reports on the miniaturization of optical traps on a planar platform using either optical fibers or vertical cavity surface emitting laser (VCSEL) diodes. The first optical fiber trap was reported by Constable et al. who utilized capillary tubes to hold and position two opposing optical fibers [2]. In later work, Lyons, et al. reported on a dual-fiber trap using two lensed fibers for trapping of polystyrene beads with diameters of 3, 5, and 10 μm [3] on microscope slides. Collins, et al. reported a four-fiber optical trap mounted into micromachined Si V-grooves fabricated using standard lithographic and etching processes. Trap strength and stability for both lensed and cleaved fibers was studied [4]. More recently, Guck, et al. reported on the application of a dual, cleaved-fiber 'optical stretcher' in which the trapped cells were distorted along the optical axis due to the momentum imparted by each optical fiber [5]. VCSEL-based traps have been studied recently. Ogura, et al. demonstrated the translation of 6 μm diameter polystyrene beads by sequentially activating an 8x8 VCSEL array without involving mechanical movement [6]. Subsequent work by Flynn, et al. characterized the VCSEL trapping forces on 5 and 10 μm microspheres, red blood cells and yeast cells [7]. McGreehin, et al, presented a slightly different approach to a planar device. Their device is a GaAs/AlGaAs heterostructure with a 100 μm wide channel, wherein counter propagating lasers trap passing polymer micro spheres [8].

Apart from component miniaturization, it is also desirable to explore multi-functional trapping modules by incorporating additional optical functions such as diagnosis, sensing and actuation into the basic trapping scheme. It is conceivable such a trapping module could ultimately be integrated into a device such as a heterogeneous biochip with built-in microfluidic delivery and other non-optics based diagnosis and synthesis functionalities. Glass or plastic based optical fibers offer an attractive means to implement such a multi-functional trap. They provide a flexible means for interfacing light in and out of the chip free of alignment encumbrances and can be bonded with a high degree of precision onto a microfabricated platform. In this paper we report a four-fiber trap module on both Si and PDMS V-grooved platforms fabricated using standard microfabrication and molding methods, respectively. We demonstrate for the first time positional control and sensing, fluorescence excitation and detection of chemically treated beads. The basic demonstration also points to many areas of improvement that can further enhance the performance of the basic module.

2. Dual-fiber trap

Traditional optical tweezers utilize both gradient and scattering forces of a single, focused optical beam for trapping of objects near the beam waist. In a dual-beam optical fiber trap, two opposing beams from two fibers separated by a distance and aligned coaxially are used to form the trap [2,3]. In our experiments, the end of the fiber facing the trap is cleaved, while the other end of the fiber is pigtailed to an independently controlled laser diode source. Trapping wavelengths of 830nm and 980nm were selected, as future work will entail the use of cells and biological molecules. The literature suggests trapping wavelengths greater than 800nm are less harmful for biological applications [9]. The polystyrene beads used in our experiments have a higher index of refraction ($n_{\text{bead}}=1.65$) than the surrounding aqueous medium ($n_{\text{water}}=1.33$). The scattering and gradient forces (F_S and F_G respectively) along the axial and transverse directions are created due to multiple reflections within the polystyrene

bead and are utilized for optical trapping. In a cleaved fiber, light diverges as soon as it leaves the cleaved facet. The scattering force generated by each fiber tends to push the polystyrene bead in the direction of light propagation, while the gradient force tends to pull the bead towards its optical axis. When the bead is pulled onto the optical axis, its position along the optical axis can be adjusted by varying the power ratio of the trap light. As the power is increased in the left fiber, the scattering force also increases and the trapped bead translates to the right as shown in Fig 1.

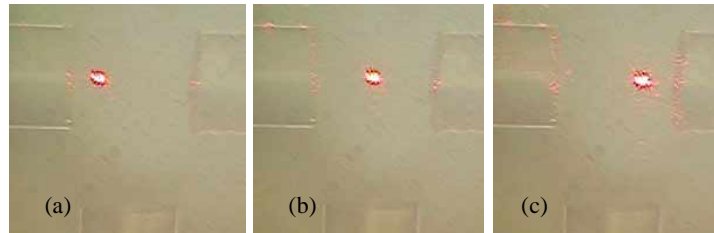


Fig. 1. As the optical power in the left fiber is increased, the scattering force increases and the trapped bead translates to the right (a \rightarrow c). The bead appears red due to the scattered 660nm trap/excitation light.

In comparison to the single-beam gradient trap, the gradient force produced by a cleaved optical fiber trap of the same power is considerably weaker due to the smaller optical gradient and the fact, in general not all of the trapping light will be intercepted by the particle. The trapping location is determined by the point where the scattering forces generated by the opposing fibers cancel each other and can be adjusted by changing the relative optical powers delivered by the trapping fibers. In terms of implementation, the optical fiber trap is a simple, robust, small-scale and low cost alternative. Since the trapping fibers are widely separated from the trapped particle, additional optical and mechanical probes can be introduced in the vicinity of the trap. For the platform material, Si was initially selected since it could be easily etched to produce V-grooves facilitating the mounting and alignment of the optical fibers. Poly dimethylsiloxane (PDMS) was selected, as it is used extensively in microfluidics, is biocompatible, is flexible and dozens of molds can be cast from a single form. Obvious benefits of PDMS over silicon include optical transparency, low cost, and high casting resolution. PDMS-based microfluidic devices such as capillary electrophoresis chips have also been widely studied [10].

3. Trap on Si platform: experiments and results

3.1 Fabrication

The basic layout of the multi-fiber trap is similar to Collin's four-fiber trap and is shown in Fig. 2(a). It consists of four right-angled V-grooves that meet to form a symmetric diamond-shaped trapping trough at the center. Two opposing V-grooves are used for mounting the trapping fibers, while the other two V-grooves are used for mounting the excitation and sensing fibers, respectively. The trap was fabricated on a Si_3N_4 coated (100) Si-wafer by first defining the pattern lithographically on the Si wafer, followed by reactive ion etching (RIE) and potassium hydroxide (KOH) etching to form the V-grooves and trough as shown in Fig. 2(b). The width of the V-grooves is designed such that when the fiber is mounted, the optical axis of the fiber is located a few microns beneath the surface of the Si wafer. The fiber is then secured in the V-groove from the surface. All trapping fibers used in this work are single-mode fibers (SMF) with diameters of $125\mu\text{m}$. The fibers were first stripped of their plastic jackets, cleaved, and mounted into the V-grooves using UV-curable adhesive. The fibers were then covered with microscope slides and UV-cured. The two trapping fibers were separated

by a distance ranging from $130\mu\text{m}$ to $170\mu\text{m}$. The overall trap size was selected for ease of handling and assembly, and could otherwise be made substantially smaller than the 2cm by 2cm size shown in Fig. 2(a).

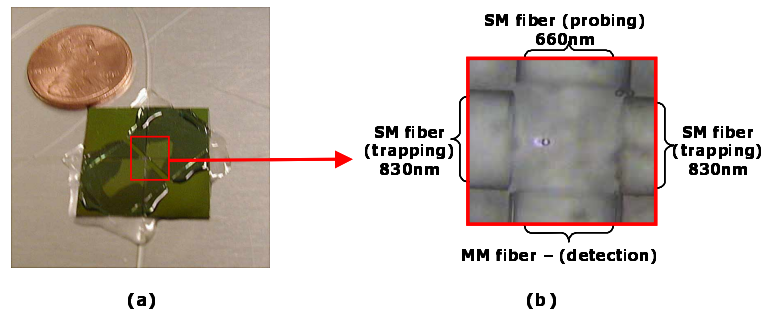


Fig. 2. The silicon platform optical trap (a) consists of four orthogonal fibers. A magnified view of the optical trap (b) reveals the trapping area between the four, cleaved fibers with a single, optically trapped bead.

3.2 Experiment

The optical trap was placed under an optical microscope with a viewing CCD camera. The two trapping fibers were connected via FC connectors to two Hitachi HL8325G pigtailed laser diodes with maximum facet powers of 40mW, emitting at 830nm. The excitation fiber, also single-mode, was pigtailed to a laser diode with a facet power of 30mW, emitting at 660nm. A multi-mode fiber was used for detection because of its larger core diameter for improved light collection. It was placed opposite the excitation fiber, and was connected to a mini-spectrometer (Ocean Optics S2000) operating with a spectral range of 350 to 1000nm and a resolution of 1nm. Two types of multi-mode fibers were used for signal detection: a graded-index fiber with a core diameter and N.A. of $62.5\mu\text{m}$ and 0.275 respectively, and a step-index fiber with a core diameter and N.A. of $100\mu\text{m}$ and 0.20 respectively. Polystyrene beads with diameters of $6\mu\text{m}$ and $10\mu\text{m}$, suspended in an aqueous solution were loaded into the trough using a syringe. The spectrometer collected both the transmitted light from the excitation fiber and the scattered light (at near right angles) from the trapping fibers. Once a bead drifted towards the optical axis and was trapped, we fine-tuned its position along the optical axis by varying the power ratio of the trapping lasers. Usually, this was done by varying the power of one of the trapping laser while keeping the other constant. When we varied the position of the bead, we recorded both the measured spectra from the detection fiber and its corresponding position as viewed under the CCD camera.

3.3 Motional Control and Sensing

Figures 3(a) and (b) show the spectra at various positions for a $6\mu\text{m}$ bead along the optical axis of the trapping fiber. The spectra clearly show wavelength peaks at 660nm and 830nm from the excitation and trapping lasers respectively. The intensity of these two peaks changed in a complementary way as the bead was moved. That is, an increase in the 660nm peak intensity is accompanied by a decrease in the intensity for the 830nm peak and vice versa. This can be understood qualitatively as follows: When the bead moved towards the center position of the detection fiber, the transmitted light from the excitation laser is reduced as the excitation light is increasingly obstructed by the bead. However, the scattered light from the trapping lasers increased steadily as more scattered light from the bead was being collected. The trap was less stable for the $10\mu\text{m}$ bead compared to the $6\mu\text{m}$ bead. This has been previously observed [11] and is attributed to a difference in the scattering force on the $10\mu\text{m}$

bead at the extreme ends of the trapping area compared to the center of the trap. For example, as the larger 10 μm bead is translated closer to one of the cleaved fiber ends where the beam is less divergent, it intercepts a smaller and smaller cross-section of the beam. In accordance with the ray optics model of trapping developed by Ashkin, it is the high angle of incidence rays striking the bead, which create the greatest force. As the beam diameter decreases, the bead intercepts fewer rays of high incidence; consequently, the scattering efficiency decreases. If greater trap stability for the 10 μm beads was required, this could have been improved by using a wider spacing between the fiber cleaves. In the case of the 6 μm bead, one could adjust the trapping power to bring the bead within a few microns of the cleaved fiber.

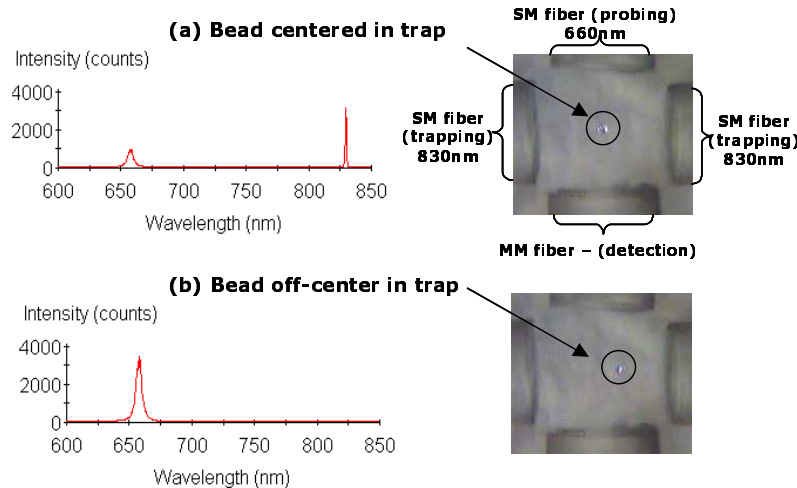


Fig. 3. Optical spectrometer data (a) indicating 660nm probing light and 830nm trapping light scattered by an optically trapped bead located at the center of the trap. Spectrometer data (b) indicating detection of 660nm probing light only for a bead trapped off-center.

Next, we plot the integrated peak intensity for both 660nm and 830nm scattered light from Fig. 3 versus the calibrated bead position from the CCD camera reading. The results are shown in Figure 4 for the 10 μm beads detected by the 100 μm and the 62.5 μm core diameter fibers, respectively. From the plot, it can be seen that the position of the trapped bead correlates well with the intensity ratio of the scattered trapping light to the transmitted excitation light. The spatial resolution of the detection was also notably higher for the 62.5 μm core fiber compared to the 100 μm core detection fiber due to its smaller aperture size. The spatial resolutions for the 6 μm and 10 μm beads however, are nearly identical. We estimate the spatial resolution of the position sensing scheme, when fully calibrated is on the order of 1 μm , superior to a CCD mounted microscope and offers much improved mechanical stability at the same time. The position sensing scheme can also be sped up for automatic position control of the trapped bead if we replace the spectrometer with a wavelength-dependent fiber coupler, each connected to a photodetector for separate detection of the trapping and excitation light.

4. Polymer platform: experiment and results

4.1 Fabrication

A replica version of the Si V-groove platform was fabricated on a PDMS (Dow Corning Sylgard 184 silicone) polymer platform using a double-molding technique [12]. The PDMS was mixed in a ratio of 10:1 prepolymer to curing agent and degassed under vacuum. A

negative PDMS master mold was first formed on a previously fabricated Si platform at a curing temperature between 80 °C to 100°C for 5 to 10 minutes. This negative mold was then mounted on glass and used as the final mold for casting the PDMS V-groove trap. For a 1mm thick PDMS sample mounted on 1.5mm thick water white glass, 90 percent transmission was observed from 350nm to 1000nm. A total of three optical fibers, two for trapping and one for detection were mounted on the finished PDMS trap. Fig. 5(a) shows the finished trap on the PDMS platform. The entire trap measured approximately 2cm by 2 cm.

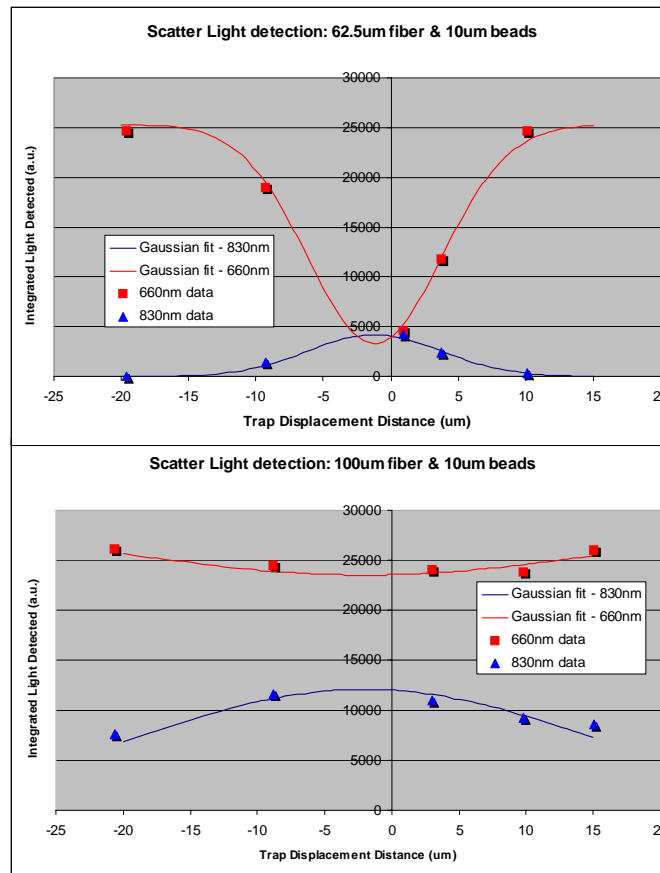


Fig. 4. Integrated peak values for light scattered from a trapped bead (830nm) and excitation light (660nm). As the bead is translated across the trap region, the scattered trap light and excitation light change in a complementary manner. Also note, the spatial resolution is greater for the 62.5 μ m (bottom) collection fiber in comparison to the 100 μ m (top) fiber.

4.2 Experiment

Two fiber trap configurations were studied for the PDMS platform as shown in Fig. 5(b). In the first configuration, the two opposing trapping fibers were connected to an E-TEK LDPM 980nm laser diode with an output of up to 90mW and a Hitachi HL6501G 660nm laser diode with a facet power of 30mW, respectively. In this configuration the 660nm laser was used for *both* trapping and fluorescence excitation of the bead. In the second configuration, the 660nm trapping laser was replaced by a pigtailed Hitachi HL8325G 830nm laser diode with a facet power of 40mW. The 660nm laser was used as an independent fluorescence excitation source and was mounted underneath the trough pointing upwards. In both configurations, a multi-

mode graded-index fiber (core diameter of $62.5\mu\text{m}$ and a NA of 0.275) was mounted at right angles to both trapping lasers and was connected to a mini-spectrometer. The high transparency of PDMS offers another way for compact 3-D integration of chip-based components such as VCSELs, photodetector arrays and thin-film filters for fluorescence excitation and detection (both position and fluorescence) respectively.

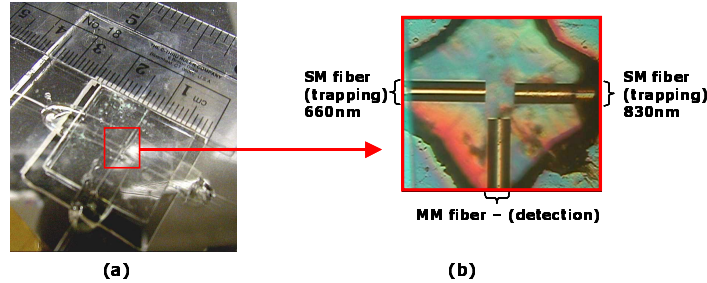


Fig. 5. The polymer platform optical trap (a) consisting of three orthogonal fibers mounted with optical adhesive and glass coverslips. A magnified view of the optical trap (b) reveals the trapping area between the cleaved fibers.

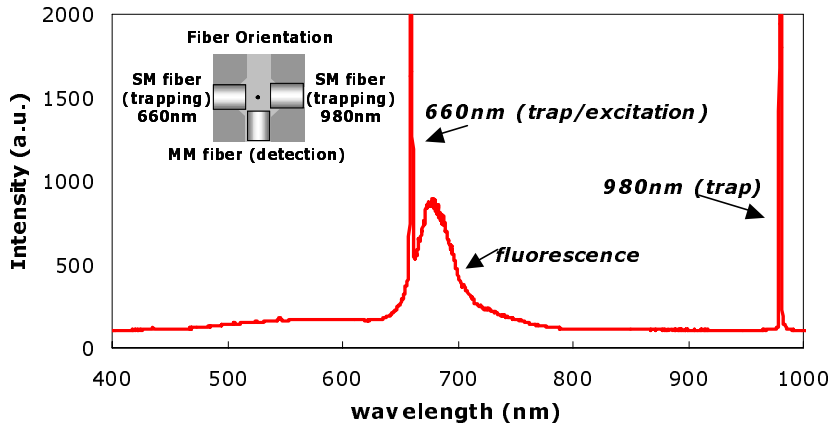


Fig. 6. Optical spectrometer data for the scattered light from a single, trapped, chemically treated bead. In this configuration, a 980nm laser and a 660nm laser are used to trap the bead. The 660nm trapping laser also serves as an excitation source, causing the trapped bead to fluoresce. Fiber orientation of the trap is provided for reference (inset).

4.3 Fluorescence detection of a trapped bead

To demonstrate simultaneous trapping and fluorescence detection, chemically treated polystyrene beads were loaded into the trap. The beads have broad fluorescence emission at 670-720nm when excited by an optical source at wavelengths between 645-660nm. After a trapped bead was confirmed by the viewing CCD camera, spectra from the detection fiber were taken. The measured spectra from an optically trapped bead using the first trap configuration is shown in Fig. 6, where the scattered trapping light, the excitation light and the fluorescence emission were clearly observed. The trap orientation is shown in the inset of Fig. 6.

The measured spectra for the second orientation, where the 660nm excitation laser was placed beneath the transparent polymer trap, are shown in Fig. 7. Again, in these spectra the fluorescence emission near 680nm can be clearly seen. These experiments demonstrate the ability of trapping and fluorescence excitation and detection using a multi-fiber trap on a biocompatible and transparent platform. In both configurations, the peak of the scattered light from the trapping laser changes with the position of the bead as observed earlier in Fig. 4. It should be noted that in both configurations, the excitation source is introduced using a cleaved SMF that suffers substantial diffraction loss. The excitation efficiency can be enhanced quite easily when an optimally focused fiber is used.

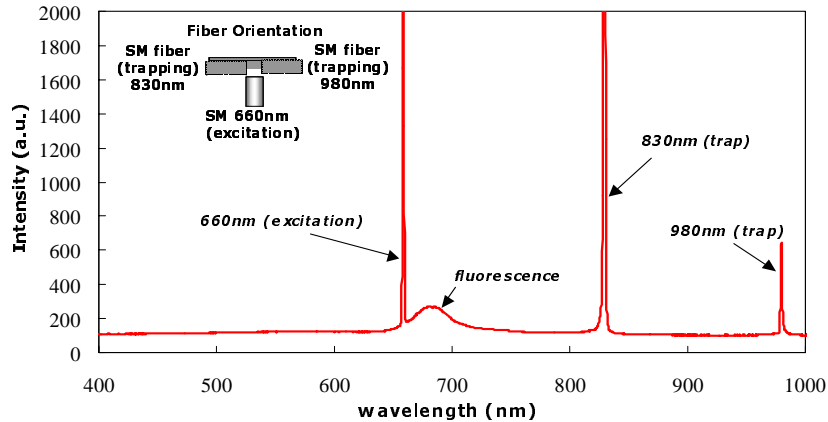


Fig. 7. Optical spectrometer data for the scattered light from a single, trapped, chemically treated bead. In this configuration, an 830nm laser and a 980nm laser are used to trap the bead. The 660nm excitation laser is positioned below the trap platform, exciting the trapped bead through the PDMS resulting in fluorescence. Fiber orientation of the trap is provided for reference (inset).

5. Areas for improvement

The demonstration of motion control, position sensing, and fluorescence excitation and detection on an optically transparent platform presents opportunities for improvement. For example, the excitation and trapping fibers can be replaced using a single VCSEL (or VCSEL arrays) mounted below the trapping trough. Two detection fibers, one multi-mode for fluorescence detection and a single-mode fiber for positional sensing can also be used to independently optimize the efficiency and spatial resolution of the fluorescence detection and positional sensing, respectively. By using smaller diameter fiber, it is possible to incorporate additional trapping and sensing fibers for two-dimensional motion and potentially spatially resolved fluorescence detection.

6. Conclusion

In summary, we demonstrate a multi-functional optical fiber trap for motion control, position sensing and fluorescence detection of chemically treated beads. On a four-fiber Si trap, we demonstrated position dependence of scattered and transmitted lights of a trapped object (bead). This sensing mechanism can be utilized for automating the positional control of the optical fiber trap. In the three-fiber PDMS optical trap, we demonstrated fluorescence excitation and detection of chemically treated and trapped beads in two geometries, including excitation through the optically transparent PDMS from the bottom of the trap. In view of the recent advances in microfluidic systems on planar substrates, the present work shows the

promise of extending the functionality of microfluidic devices and systems through the use of optical fiber traps.